Learning-based Adaptive Gust Mitigation with Oscillating Wings

Naresh Poudel, * Arjun Trivedi, † Parham Oveissi‡ Meilin Yu, and § Ankit Goel¶
Department of Mechanical Engineering, University of Maryland Baltimore County

John T. Hrynuk‖
DEVCOM – Army Research Lab, Aberdeen Proving Ground

This paper investigates the application of a learning-based adaptive controller to mitigate the effect of gust on the lift generated by an airfoil in an unsteady flow environment. A high-order accurate CFD model is used to model the unsteady flow over a pitching airfoil. Open-loop simulations of the CFD model are used to ascertain feasible lift commands. The learning-based adaptive controller is based on the retrospective cost adaptive control (RCAC). First, RCAC is used to regulate the lift coefficient of the airfoil in a nominal case without gust. Next, the effect of the hyperparameters of the adaptive control on the closed-loop performance is investigated. Finally, we used RCAC to regulate the lift coefficient and mitigated the effect of gust on the airfoil.

Nomenclature

t^*	=	non-dimensional time
α	=	angle of attack
r_k	=	command at step k
y_k	=	measured output at step k
z_k	=	error signal at step k
u_k	=	controller output at step k
θ_k	=	controller coefficients at step k

I. Introduction

Unmanned aerial vehicles (UAVs) often encounter highly unsteady flows, such as gusts, with widely separated spatiotemporal scales. These harsh flow conditions negatively affect the performance of UAVs, even severely restricting their operating environments. To overcome the negative influence imposed by unsteady gusts, both active and passive flow control techniques, based on *in situ* flow conditions, need to be developed. However, designing such a control system for effective gust mitigation is a challenging problem due to highly transient, high-dimensional, and nonlinear flow physics of the gust-vehicle interactions.

Various studies have demonstrated the potential of oscillating wing motion for mitigation of the gust-induced negative effects [1–10]. These early results indicate that oscillating wing motions generate flow structures that inhibit the random flow separation inherent in typically stalled wings. However, the conditions needed to reject gust-induced stall or the flow structures that inhibit traditional stall behaviors are not well understood. This problem motivates us to consider the use of adaptive techniques to mitigate the negative impact of gust. Specifically, we investigate the application of retrospective cost adaptive control (RCAC) to regulate the lift generated by a wing structure in presence of gust effects. A key feature of RCAC that makes it particularly attractive to flow-control problems is its ability to adapt online as necessary. Furthermore, since RCAC requires only measured data (and not a system model) to optimize the

*Postdoctoral Researcher, Department of Mechanical Engineering, 1000 Hilltop Circle, Baltimore, MD 21250. npoudel1@umbc.edu
†Undergraduate Student, Department of Mechanical Engineering, 1000 Hilltop Circle, Baltimore, MD 21250. atrived2@umbc.edu
‡Graduate Student, Department of Mechanical Engineering, 1000 Hilltop Circle, Baltimore, MD 21250. parhamo1@umbc.edu
§Associate Professor and AIAA Senior Member, Department of Mechanical Engineering, 1000 Hilltop Circle, Baltimore, MD 21250. mlyu@umbc.edu
¶Assistant Professor, Department of Mechanical Engineering, 1000 Hilltop Circle, Baltimore, MD 21250. ankgoel@umbc.edu
‖Mechanical Research Engineer, Weapons and Materials Research Directorate, DEVCOM Army Research Lab, MD, 21005. john.t.hrynuk.civ@army.mil

controller, it can be directly integrated with a numerical simulation for purposes of training and stress testing. These features enable RCAC to be tuned using a computationally simple simulation of the system, and to then adapt in an appropriate way to a more realistic simulation, or to the physical system itself. RCAC has been previously applied to the problem of regulating thrust in a scramjet engine in presence of unknown and unmodeled disturbances [11–13].

In this paper, we investigate the application of RCAC to regulate the lift generated by an airfoil in presence of gust using only the input and measured output data. A high-order accurate CFD model [14–17] is used to model unsteady flow over a pitching airfoil. The main contribution of this work is the demonstration of model-free, learning-based, adaptive regulation of the lift generated by an airfoil in presence of gust, without any analytical modeling information. The paper is organized as follows. Section II describes the pitching wing model used to simulate the unsteady flow over a pitching wing, Section III briefly reviews the RCAC algorithm, and Section IV presents the numerical simulations showing arbitrary regulation of lift coefficient and mitigation of gust effects. Finally, the paper concludes with a discussion of the results in Section V.

II. Pitching Wing Model

This section briefly describes the numerical model and the gust generation mechanism used in this work. A high-order accurate computational fluid dynamics (CFD) solver based on unstructured moving/deformable grids [14–17] is used to simulate unsteady flows over a pitching airfoil. This numerical framework has been extensively validated with experiments [8–10], and has been used to investigate unsteady flapping wing aerodynamics over a broad range of flow conditions [18–22]. Readers are referred to [15, 17] for more technical details about the numerical framework.

The transient gust in this study is generated by a cross-flow ducted floor jet, and its interaction with the freestream flow caused the jet to bend downstream, creating a blockage effect and changing the effective angle of attack (AoA) over the airfoil in the freestream flow. In all simulations, the gust ratio (GR) was set to 0.42, which is defined as the gust's vertical speed divided by the freestream velocity (i.e. V/U_∞). The details of the numerical modeling and gust-airfoil interaction flow physics can be found in [8–10]. Figure 1 shows a nominal instantaneous vorticity field in a gust-wing interaction at Reynolds number 1,000. Once the gust has fully developed, it is observed that the NACA0012 airfoil experiences a large change in AoA, resulting in highly unsteady behavior. Note that $t^* \triangleq tU_\infty/c$ is the non-dimensional time.

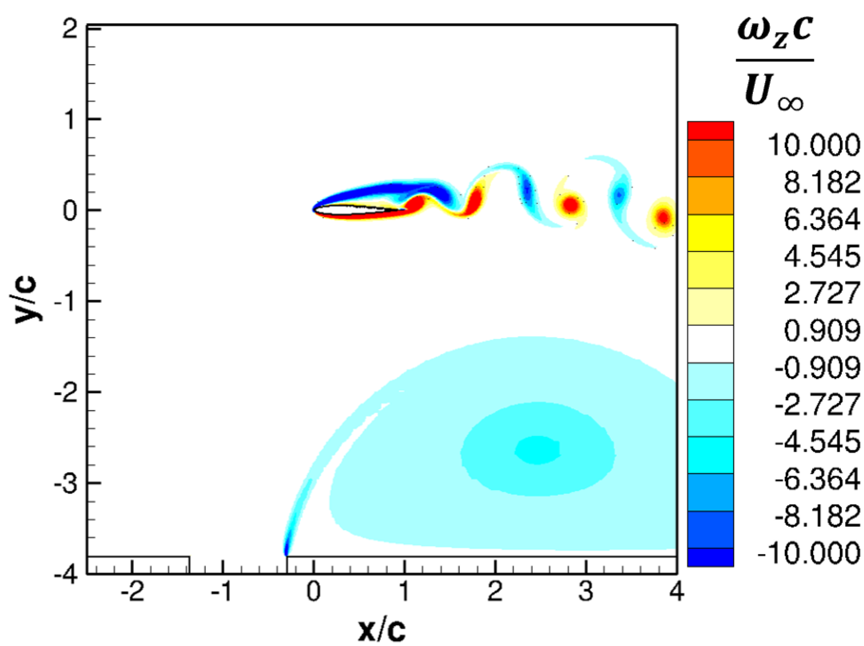

Fig. 1 Instantaneous vorticity field around the airfoil at $t^* = 64$ during the gust-wing interaction at Re = 1, 000.

III. RCAC Algorithm

This section briefly reviews the retrospective cost adaptive control (RCAC) algorithm. RCAC is described in detail in [23] and its extension to digital PID control is given in [24]. Consider a system

$$x_{k+1} = f(k, x_k, u_k, w_k), \tag{1}$$
$$y_k = g(k, x_k, w_k), \tag{2}$$

where $x_k \in \mathbb{R}^{l_x}$ is the state, $u_k \in \mathbb{R}^{l_u}$ is the input, $y_k \in \mathbb{R}^{l_y}$ is the measured output, and $w_k \in \mathbb{R}^{l_w}$ is the exogenous signal that can represent commands, external disturbance, or both. The functions f and g represent the dynamics map and the output map. The goal is to develop an adaptive control law that drives the output y_k to a desired values with limited modeling information about (1), (2). Note that explicit knowledge of f and g is not assumed since RCAC requires only the input and output measurements.

Consider a linearly parameterized control law

$$u_k = \Phi_k \theta_k, \tag{3}$$

where $\Phi_k \in \mathbb{R}^{l_u \times l_\theta}$ is the regressor matrix that is constructed using the measured data and $\theta_k \in \mathbb{R}^{l_\theta}$ is the vector of the controller coefficients optimized by RCAC at step k. For example, a discrete-time PID control law can be written in the regressor form given by (3), where, at step k,

$$\Phi_k \triangleq \begin{bmatrix} z_k & \gamma_k & z_k - z_{k-1} \end{bmatrix}, \theta_k = \begin{bmatrix} K_{\mathrm{p},k} \\ K_{\mathrm{i},k} \\ K_{\mathrm{d},k} \end{bmatrix}, \tag{4}$$

$\gamma_k = \sum_i z_i$ is the accumulated error, and $K_{\mathrm{p},k}, K_{\mathrm{i},k}$, and $K_{\mathrm{d},k}$ are the proportional, integral, and derivative gains, respectively. Various MIMO controller parameterizations of the control law (3) are given in [25]. To determine the controller gains θ_k, let $\theta \in \mathbb{R}^{l_\theta}$, and consider the *retrospective performance variable* defined by

$$\hat{z}_k(\theta) \triangleq g(z_k) + G_{\mathrm{f}}(\mathbf{q})(\Phi_k \theta - u_k), \tag{5}$$

where

$$G_{\mathrm{f}}(\mathbf{q}) \triangleq \sum_{i=1}^{n_{\mathrm{f}}} \frac{N_i}{\mathbf{q}^i} \tag{6}$$

is an FIR filter. Note that $N_i \in \mathbb{R}^{l_z \times l_u}$. Furthermore, define the *retrospective cost function* $J_k \colon \mathbb{R}^{l_\theta} \to [0, \infty)$ by

$$J_k(\theta) \triangleq \sum_{i=0}^{k} \hat{z}_i(\theta)^{\mathrm{T}} R_z \hat{z}_i(\theta) + (\Phi_k \theta)^{\mathrm{T}} R_u (\Phi_k \theta) + (\theta - \theta_0)^{\mathrm{T}} P_0^{-1} (\theta - \theta_0), \tag{7}$$

where $R_z \in \mathbb{R}^{l_z \times l_z}$, $R_u \in \mathbb{R}^{l_u \times l_u}$, and $P_0 \in \mathbb{R}^{l_\theta \times l_\theta}$ are positive definite; and $\theta_0 \in \mathbb{R}^{l_\theta}$ is the initial vector of controller gains.

Proposition III.1 *Consider (7), where $\theta_0 \in \mathbb{R}^{l_\theta}$ and $P_0 \in \mathbb{R}^{l_\theta \times l_\theta}$ is positive definite. For all $k \geq 0$, denote the minimizer of J_k given by (7) by*

$$\theta_{k+1} \triangleq \underset{\theta \in \mathbb{R}^n}{\operatorname{argmin}}\, J_k(\theta). \tag{8}$$

Then, for all $k \geq 0$, θ_{k+1} is given by

$$\theta_{k+1} = \theta_k - P_{k+1} \Phi_{\mathrm{f},k}^{\mathrm{T}} R_z \left(z_k + \Phi_{\mathrm{f},k} \theta_k - u_{\mathrm{f},k} \right) - P_{k+1} \Phi_k^{\mathrm{T}} R_u \Phi_k \theta_k, \tag{9}$$

where

$$P_{k+1} = P_k - P_k \overline{\Phi}_k^{\mathrm{T}} \left(\overline{R}^{-1} + \overline{\Phi}_k P_k \overline{\Phi}_k^{\mathrm{T}} \right)^{-1} \overline{\Phi}_k P_k, \tag{10}$$

and

$$\Phi_{\mathrm{f},k} \triangleq G_{\mathrm{f}}(\boldsymbol{q}) \Phi_k, \quad u_{\mathrm{f},k} \triangleq G_{\mathrm{f}}(\boldsymbol{q}) u_k, \quad \overline{\Phi}_k \triangleq \begin{bmatrix} \Phi_{\mathrm{f},k} \\ \Phi_k \end{bmatrix}, \quad \overline{R} \triangleq \begin{bmatrix} R_z & 0 \\ 0 & R_u \end{bmatrix}. \tag{11}$$

Proof: See [26]

Finally, the control is given by

$$u_{k+1} = \Phi_{k+1}\theta_{k+1}. \tag{12}$$

IV. Simulation Results

This section presents the implementation and performance of the learning controller to mitigate the detrimental effect of gust on an airfoil in an unsteady flow environment. The control system architecture to control the lift produced by the airfoil in the presence of gust-generated disturbances is shown in Figure 2. The commanded lift coefficient is denoted by r, and the lift generated by the airfoil is denoted by y. The error signal $z \triangleq y - r$ is used to update the RCAC control law as well as drive the RCAC controller to generate controller output u, which is the pitch angle of the airfoil. The disturbance signal d is the gust. Note that RCAC does not require or use the disturbance signal to update the control law.

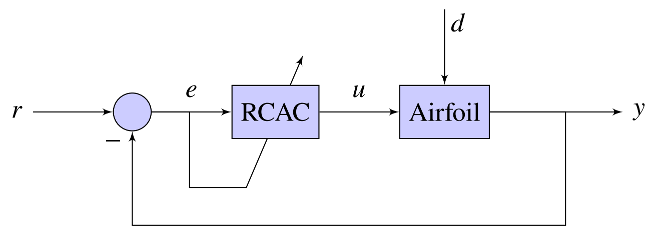

Fig. 2 Control architecture to regulate the lift coefficient as well as mitigate the effect of unknown gust.

In order to determine feasible lift coefficient commands, we simulate the flow around the airfoil without gust. A command is *feasible* if there exists a constant input, the pitch angle in this case, such that the output converges to the commanded value asymptotically. This is the *open-loop simulation* of the flow. Figure 3 shows the open-loop simulation where the pitch angle is increased/decreased by 2 degrees after the flow structure converges. Note that the lift coefficient converges to constant values for pitch angle $\alpha \leq 8$ degrees. For pitch angle $\alpha \geq 8$ degrees, vortices are shed at a frequency that depends on the flow parameters, and thus, the lift coefficient oscillates and does not converge to a steady value.

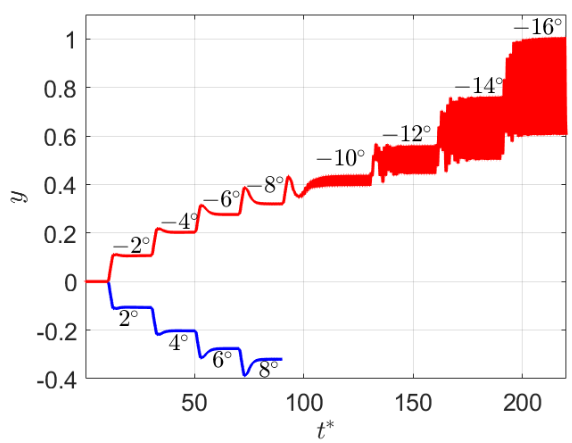

Fig. 3 Open-loop lift coefficient for various values of pitch angles.

Next, we use RCAC to regulate the lift generated by the airfoil in the absence of gust. We consider this case to demonstrate that the learning controller is indeed able to follow the desired commands in nominal cases as well as tune the hyperparameters of the RCAC algorithm. The airfoil is commanded to generate a lift coefficient value of $r = 0.1$ for $t^* \in (0, 10)$ and $r = 0.2$ for $t^* \in (10, 20)$, where t^* is the normalized time. We use an adaptive PID control law, where the proportional, integral, and the derivative gains, K_p, K_i, and K_d, respectively, are updated by the RCAC algorithm described in Section III. In the algorithm, we set $P_0 = 10^{-1} I_3$, $R_u = 0$, $N_1 = -1$, and $\theta_0 = 0$. Figure 4 shows the closed-loop response, a) shows the commanded and the generated lift coefficient, b) shows the pitching angle updated by RCAC, c) shows the absolute value of the error signal on a log scale, and d) shows the controller gains updated by RCAC at each step. Note that RCAC updates the control law (3) using only the error signal z_k and past control u_k. Figure 5 shows the instantaneous vorticity field at two instants verifying that the flow has indeed converged. Figures 4 and 5 show that RCAC is able to adaptively regulate the lift coefficients by concurrently learning the controller coefficients using only the measured data without requiring any modeling information or freestream flow parameters.

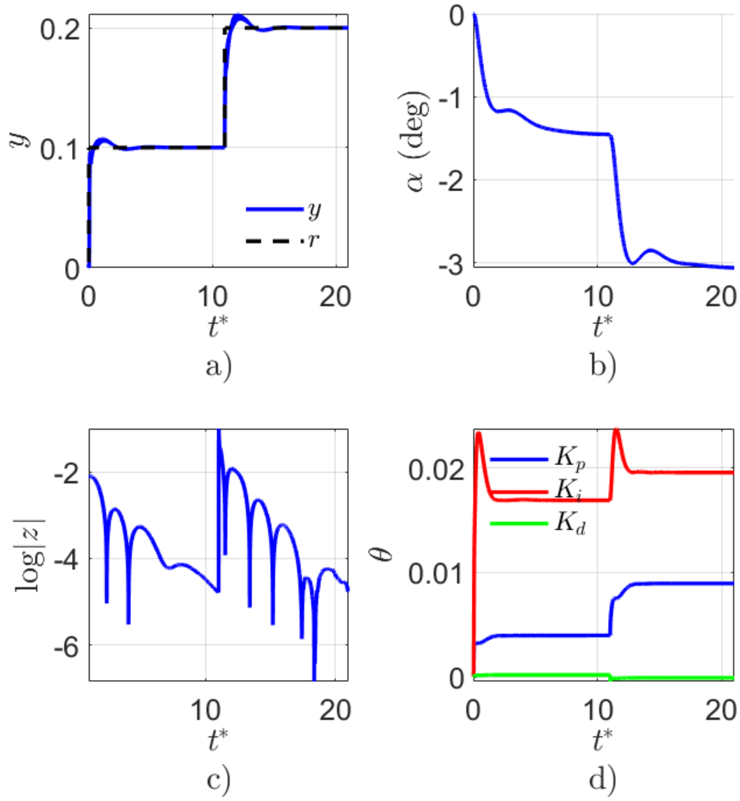

Fig. 4 Closed-loop response of the Airfoil to constant lift commands.

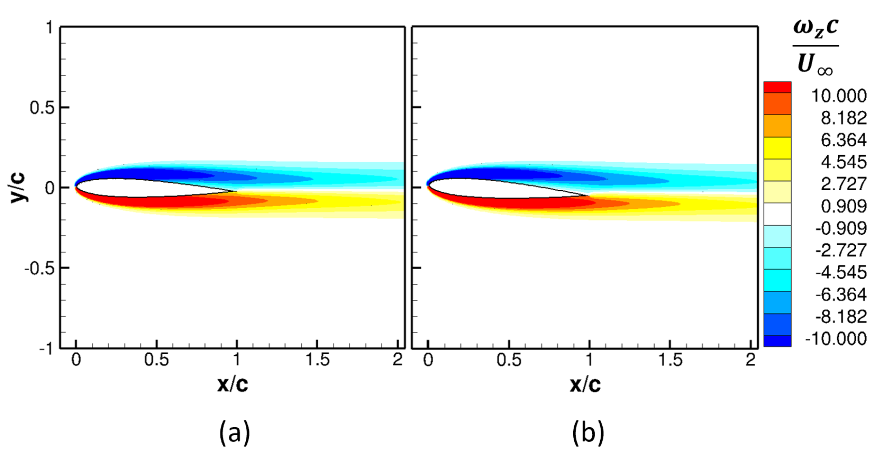

Fig. 5 Instantaneous vorticity fields (a) at $t^* = 10$ and (b) $t^* = 20$ in the closed-loop simulation.

Figure 6 shows the effect of RCAC hyperparameters on the closed-loop response of the airfoil. Note that as P_0

increases, overshoot decreases, and as N_1 increases, the settling time decreases. Finally, note that the closed-loop response is not very sensitive to the RCAC hyperparameters as they can be varied by as much as two orders of magnitude while maintaining acceptable closed-loop response.

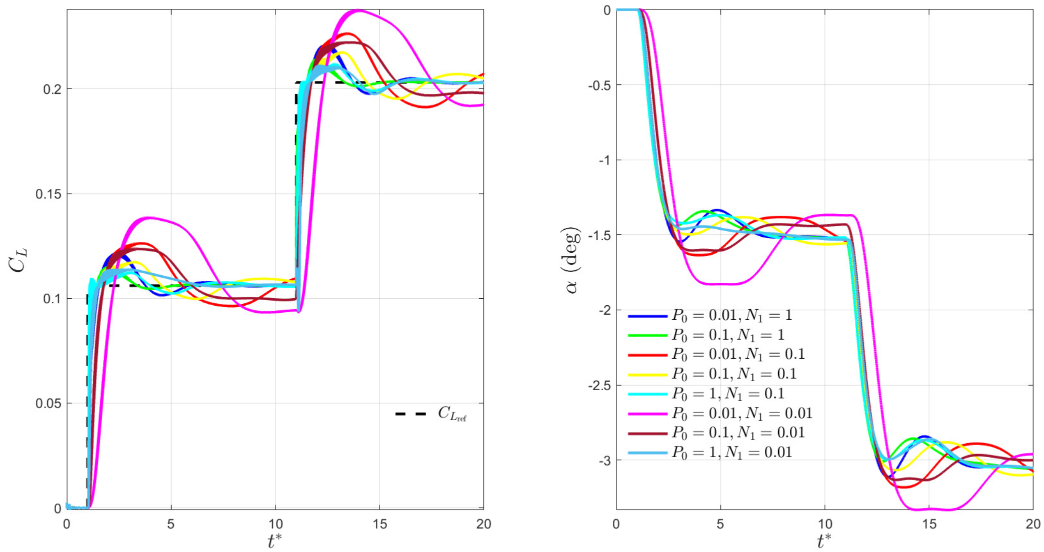

a) b)

Fig. 6 Effect of RCAC's hyperparameters P_0 and N_1 on the closed-loop response of the Airfoil to constant lift commands.

Finally, we consider the problem of mitigating the effect of gust in an unsteady flow environment as described in Section II. The gust generation mechanism is described in Section II. The stationary airfoil experiences highly unsteady events as the gust grows over time due to the change in effective angle of attack caused by the gust as shown in Figure 1.

Figure 7 shows the lift coefficient response of the airfoil in an unsteady environment caused by gust. In Figure 7a), the red trace shows the open-loop lift coefficient response in the case where the airfoil pitch is fixed at 0 degrees. The blue trace shows the closed-loop loop response. In the closed-loop simulation, we switch on RCAC at $t^* = 20$. RCAC is switched on after a delay to allow the gust structure to form fully and numerical transients to decrease. This time period is shown by the shaded yellow region. Figure 7c) shows the output error on a logarithmic scale and Figure 7d) shows the PID gains of the controller optimized by RCAC. Once RCAC is switched on at $t^* = 20$, the airfoil pitch is modulated by the controller to mitigate the effect of gust. In this case, the lift coefficient is commanded to a value of $r(t^*) = 0.1$ for $t^* \in (20, 40]$ and $r(t^*) = 0.2$ for $t^* \in (40, 60]$. Note that the RCAC hyperparameters are not retuned when the gust is switched on. Figure 8 shows the instantaneous vorticity fields obtained in the open-loop and the closed-loop simulation at two time instants; a) and c) show the open-loop vorticity fields at $t^* = 25$ and $t^* = 45$, respectively, and b) and d) show the closed-loop vorticity fields at $t^* = 25$ and $t^* = 45$, respectively. In closed-loop, that is, with the learning controller controlling the pitch angle of the airfoil, the learning controller automatically finds the correct pitch angle to generate the desired lift coefficient despite the presence of gust. This numerical simulation demonstrates that RCAC-based learning controller is capable of both regulating the lift and mitigating the oscillatory effect of gust on the lift coefficient.

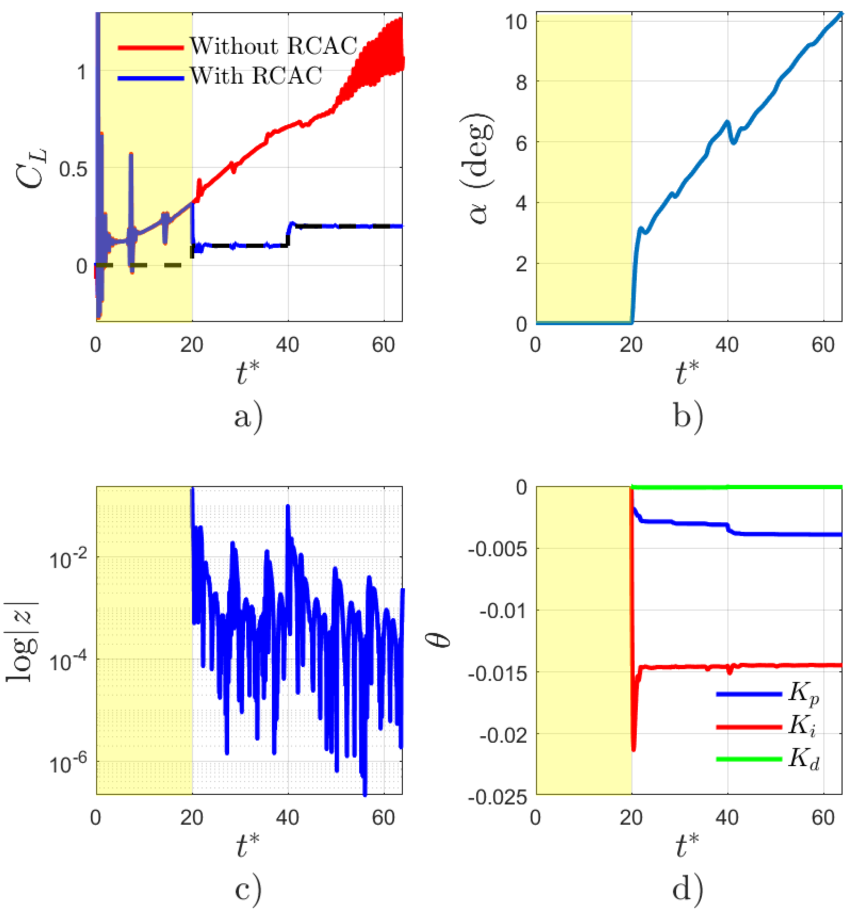

Fig. 7 Closed-loop response of the airfoil in the presence of gust.

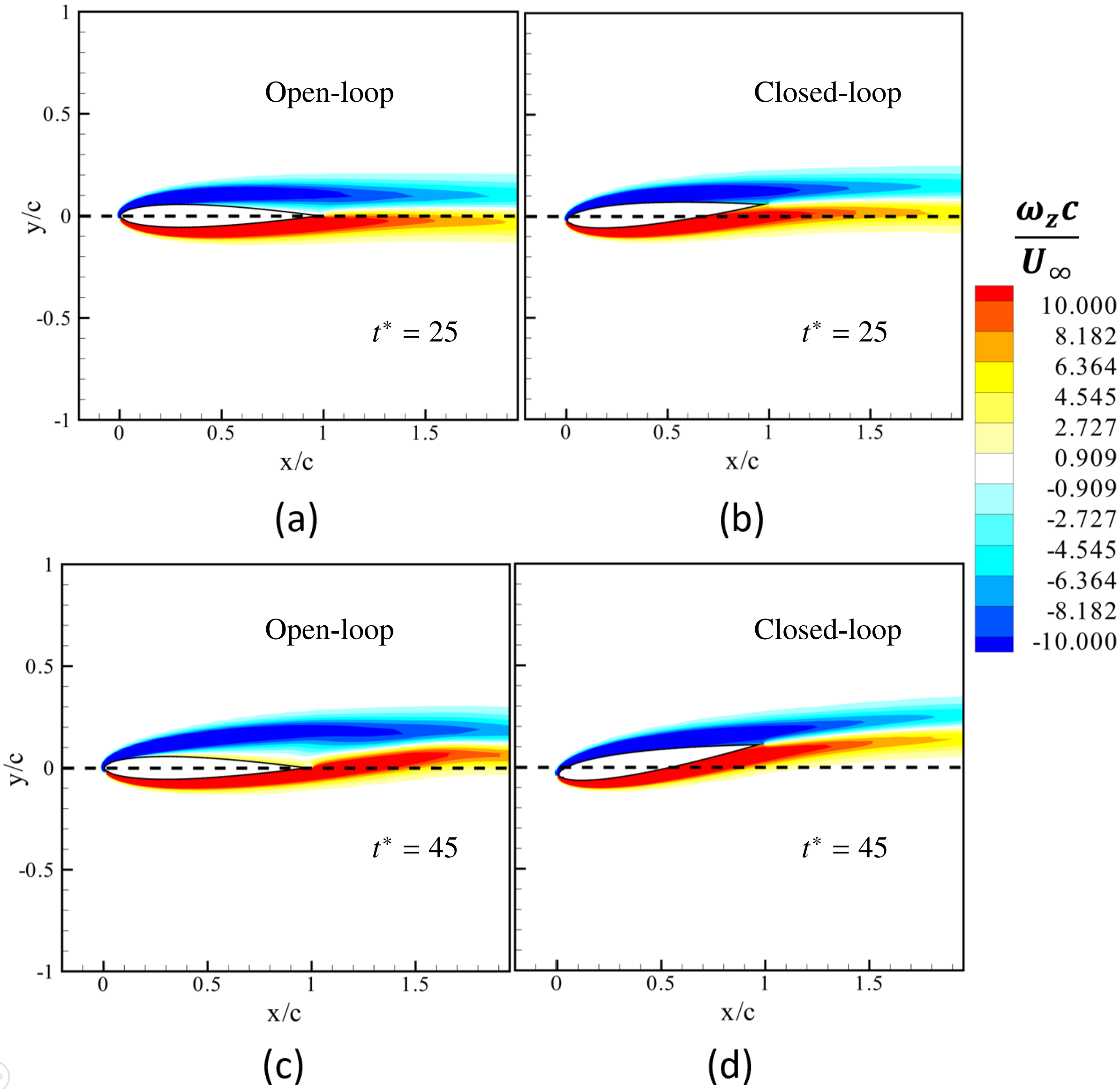

Fig. 8 Instantaneous vorticity fields obtained in the open-loop and the closed-loop simulation at two time instants. a) and c) show the open-loop vorticity fields at $t^* = 25$ and $t^* = 45$, respectively. b) and d) show the closed-loop vorticity fields at $t^* = 25$ and $t^* = 45$, respectively.

V. Conclusion

In this work, we developed and tested a control-guided flow simulation framework for gust mitigation applications. Specifically, we developed an adaptive PID controller, based on the retrospective cost adaptive control algorithm, to regulate the lift coefficient of a NACA0012 airfoil in an unsteady flow environment caused by a cross-flow gust at low Reynolds numbers. In the control-guided flow simulation framework, we used a high-order accurate CFD solver based on unstructured moving/deformable grid to simulate the unsteady flow over an airfoil capable of conducting pitching maneuver. The adaptive PID controller was then integrated with the CFD solver and tuned to obtain the desired transient performance and was shown to be robust to the hyperparameters of the learning algorithm. Different from previous relevant works, no explicit flow model is used to build the controller; instead, high-fidelity data from CFD simulations are used to train the RCAC-based controller online. From numerical experiments, we observed that only in about twice of the characteristic time, during which the flow passes one chord length of the airfoil, the RCAC-based PID controller can mitigate the gust effect to regulate lift over the airfoil. Finally, we demonstrated that the learning controller is capable of maintaining an arbitrary constant lift coefficient output in an unsteady flow environment caused by a developing gust.

We mention that the current work is the first step to demonstrate the control-guided flow simulation concept, in which flow simulation and control are seamlessly integrated to function iteratively with the aim of achieving specific control goals, such as maintaining constant lift over a wing in unknown gusts. As a byproduct, the flow physics behind adaptive control can be readily shown from flow simulation, which can in turn assist improving the controller design. In our future work, we will further test the high-fidelity control-guided flow simulation framework at higher Reynolds numbers where more complex flow structures will show up and need to be controlled.

Acknowledgments

This research was conducted at UMBC and the DEVCOM ARL contributions have been approved for public release. The hardware used in the computational studies is part of the UMBC High Performance Computing Facility (HPCF). The facility is supported by the U.S. National Science Foundation through the MRI program (grant nos. CNS-0821258, CNS-1228778, and OAC-1726023) and the SCREMS program (grant no. DMS-0821311), with additional substantial support from the University of Maryland, Baltimore County (UMBC).

References

[1] Moulin, B., and Karpel, M., "Gust loads alleviation using special control surfaces," *J. Aircr.*, Vol. 44, No. 1, 2007.

[2] Zarovy, S., Costello, M., Mehta, A., Gremillion, G., Miller, D., Ranganathan, B., Humbert, J. S., and Samuel, P., *Experimental study of gust effects on micro air vehicles*, in AIAA Atmospheric Flight Mechanics Conference, Toronto, 2010.

[3] Cook, R. G., Palacios, R., and Goulart, P., "Robust gust alleviation and stabilization of very flexible aircraft," *AIAA J.*, Vol. 51, No. 2, 2013.

[4] Bhatia, M., Patil, M., Woolsey, C., Stanford, B., and Beran, P., "Stabilization of flapping-wing micro-air vehicles in gust environments," *J. Guid. Control Dyn.*, Vol. 37, No. 2, 2014.

[5] Perrotta, G., and Jones, A. R., "Unsteady forcing on a flat-plate wing in large transverse gusts," *Experiments in Fluids*, Vol. 58, No. 101, 2017.

[6] Smith, Z. F., Jones, A. R., and Hrynuk, J. T., *Micro Air Vehicle Scale Gust-Wing Interaction in a Wind Tunnel*, in 2018 AIAA Aerospace Sciences Meeting, AIAA SciTech Forum, 2018-0573, 2018.

[7] Corkery, S. J., Babinsky, H., and Harvey, J. K., "On the development and early observations from a towing tank-based transverse wing–gust encounter test rig," *Experiments in Fluids*, Vol. 59, 2018, p. 135.

[8] Poudel, N., Yu, M. L., Smith, Z. F., and Hrynuk, J. T., *A combined experimental and computational study of a vertical gust generator in a wind tunnel*, in AIAA Scitech 2019 Forum, AIAA-2019-2166, San Diego, California, 2019.

[9] Poudel, N., Wang, L., Yu, M. L., and Hrynuk, J. T., *Computational Study of Flapping Wing Response to Vertical Gusts at Low Reynolds Numbers*, in AIAA Scitech 2020 Forum (AIAA 2020-2046), Orlando, FL, 2020.

[10] Poudel, N., Yu, M., and Hrynuk, J., "Gust mitigation with an oscillating airfoil at low Reynolds number," *Physics of Fluids*, Vol. 33, 2021, p. 101905.

[11] Goel, A., Xie, A., Duraisamy, K., and Bernstein, D. S., "Retrospective cost adaptive thrust control of a 1D scramjet with Mach number disturbance," *2015 American Control Conference (ACC)*, 2015, pp. 5551–5556. https://doi.org/10.1109/ACC.2015.7172208.

[12] Goel, A., Duraisamy, K., and Bernstein, D. S., "Retrospective cost adaptive control of unstart in a model scramjet combustor," *AIAA Journal*, Vol. 56, No. 3, 2018, pp. 1085–1096. https://doi.org/10.2514/1.J055812.

[13] Goel, A., Duraisamy, K., and Bernstein, D., "Output-Constrained Adaptive Control for Unstart Prevention in a 2D Scramjet Combustor," *AIAA Scitech 2019 Forum*, 2019, p. 0927. https://doi.org/10.2514/6.2019-0927.

[14] Yu, M. L., Wang, Z., and Hu, H., "A high-order spectral difference method for unstructured dynamic grids," *Computers & Fluids*, Vol. 48, 2011, pp. 84–97.

[15] Yu, M. L., Wang, Z. J., and Liu, Y., "On the accuracy and efficiency of discontinuous Galerkin, spectral difference and correction procedure via reconstruction methods," *J. Comput. Phys*, Vol. 259, 2014, pp. 70–95.

[16] Wang, L., and Yu, M. L., "An Implicit High-Order Preconditioned Flux Reconstruction Method for Low-Mach-Number Flow Simulation with Dynamic Meshes," *International Journal for Numerical Methods in Fluids*, Vol. 91, 2019, pp. 348–366.

[17] Wang, L., Gobbert, M., and Yu, M. L., "A dynamically load-balanced parallel p-adaptive implicit high-order flux reconstruction method for under-resolved turbulence simulation," *Journal of Computational Physics*, Vol. 417, 2020, p. 109581.

[18] Yu, M. L., Wang, Z. J., and Hu, H., "Airfoil thickness effects on the thrust generation of plunging airfoils," *Journal of Aircraft*, Vol. 49, No. 5, 2012, pp. 1434–1439.

[19] Yu, M. L., Wang, Z. J., and Hu, H., "Formation of bifurcated wakes behind finite-span flapping wings," *AIAA Journal*, Vol. 51, No. 8, 2013, pp. 2040–2044.

[20] Yu, M. L., Wang, Z., and Hu, H., "High fidelity numerical simulation of airfoil thickness and kinematics effects on flapping airfoil propulsion," *Journal of Fluids and Structures*, Vol. 42, 2013, pp. 166–186.

[21] Yu, M. L., Wang, Z. J., and Hu, H., "Numerical optimization of flapping foil kinematics using high order spectral difference method," *Acta Aerodynamica Sinica*, Vol. 32, 2014, pp. 727–740.

[22] Yu, M. L., Wang, B., Wang, Z. J., and Farokhi, S., "Evolution of vortex structures over flapping foils in shear flows and its impact on aerodynamic performance," *Journal of Fluids and Structures*, Vol. 76, 2018, pp. 116–134.

[23] Rahman, Y., Xie, A., and Bernstein, D. S., "Retrospective Cost Adaptive Control: Pole Placement, Frequency Response, and Connections with LQG Control," *IEEE Control System Magazine*, Vol. 37, 2017, pp. 28–69. https://doi.org/10.1109/MCS.2017.2718825.

[24] Kamaldar, M., Islam, S. A. U., Sanjeevini, S., Goel, A., Hoagg, J. B., and Bernstein, D. S., "Adaptive digital PID control of first-order-lag-plus-dead-time dynamics with sensor, actuator, and feedback nonlinearities," *Advanced Control for Applications*, Vol. 1, No. 1, 2019, p. e20. https://doi.org/10.1002/adc2.20.

[25] Goel, A., U. Islam, S. A., and Bernstein, D. S., "Adaptive Control of MIMO Systems Using Sparsely Parameterized Controllers," *2020 American Control Conference (ACC)*, 2020, pp. 5340–5345. https://doi.org/10.23919/ACC45564.2020.9147513.

[26] Islam, S. A. U., and Bernstein, D. S., "Recursive Least Squares for Real-Time Implementation," *IEEE Control Systems Magazine*, Vol. 39, No. 3, 2019, pp. 82–85. https://doi.org/10.1109/MCS.2019.2900788.